

# 1 Experimental validation of the energy ship concept for far-offshore wind 2 energy conversion

3 A. Babarit<sup>a\*1</sup>, N. Abdul Ghani<sup>a,b</sup>, E. Brouillette<sup>a</sup>, S. Delvoye<sup>a</sup>, M. Weber<sup>a</sup>, A. Merrien<sup>a</sup>, M. Michou<sup>c</sup>, J-C.

4 Gilloteaux<sup>a</sup>

5 <sup>a</sup> LHEEA, Ecole Centrale de Nantes - CNRS, Nantes, France

6 <sup>b</sup> Universiti Pertahanan Nasional Malaysia, Kuala Lumpur, Malaysia

7 <sup>c</sup> Watt&Sea, La Rochelle, France

8 \* Corresponding author: aurelien.babarit@ec-nantes.fr

## 9 Abstract

10 The energy ship is a new concept for offshore wind energy capture. It consists of a wind-propelled ship  
11 that generates electricity using water turbines attached underneath its hull. Since it is not grid-  
12 connected, the generated energy is stored aboard the ship (for instance, using batteries or through  
13 conversion to hydrogen using an electrolyzer).

14 This concept has received little attention until today. Particularly, there had not been yet an  
15 experimental proof-of-concept. In order to bridge this gap, an experimental platform has been  
16 developed at Centrale Nantes. It consists of a 5.5 m long catamaran equipped with a 240 mm diameter  
17 water turbine. The platform was tested in July 2019 on the river Erdre (France). Results show that the  
18 energy ship concept can deliver high levels of power production (megawatts); and that it is essential  
19 to optimize the water turbine induced drag in order to maximize energy production.

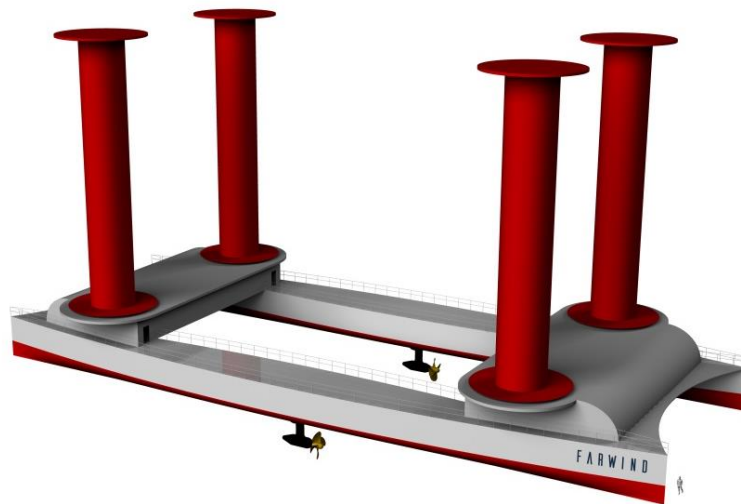
20 **Keywords:** offshore wind energy, energy ship, experiments

## 21 1. Introduction

---

<sup>1</sup> Now with Farwind Energy, 1 rue de la Noë, 44300 Nantes, France

22 Since 2017, the LHEEA lab. has been studying the energy ship concept for offshore wind energy  
23 conversion. This concept consists of a ship propelled by the wind (using sails) that generate electricity  
24 using water turbines attached underneath its hull. The electricity produced is stored on board, either  
25 in batteries or in the form of fuel (hydrogen, ammonia, methanol, etc. [1]). Figure 1 shows an artist  
26 impression of an energy ship.



27

28 *Figure 1. Artist's impression of an 80m energy ship fitted with four Flettner rotors for*  
29 *propulsion and two water turbines for converting wind speed into electricity.*

30 Despite the energy ship concept was patented in 1982 [2], it has been the matter of only a little  
31 number of studies so far [3] - [10]. Using analytical and numerical modelling, Kim & Park [3] showed  
32 that an energy ship propelled by a 3,000 m<sup>2</sup> kite could generate approximately 1.2 MW if sailing in a  
33 wind of 20 knots. In [10], we showed that in the same wind conditions, an 80 m long catamaran  
34 equipped with four 30 m high rotor sails (Flettner rotors) and two 4 m diameter water turbines could  
35 generate 1.6 MW.

36 Furthermore, Pelz et al. [5] showed that a key parameter for maximizing energy recovery is the  
37 drag induced by the water turbine. This is because the power absorbed by the water turbine is equal  
38 to the product of the induced drag times the cube of the average flow velocity across the propeller  
39 disc, which is proportional to the ship velocity. If the induced drag is very large, then the ship velocity

40 is very small, and the power absorbed tends towards zero. Conversely, if the drag is very small, the  
41 ship velocity tends towards that without the water turbine, but the power absorbed also tends towards  
42 zero. Between these two extremes, there is an optimum. We showed in [10] that this optimum can be  
43 significantly different from that for wind turbines or tidal turbines (because the input flow speed - the  
44 ship-velocity - depends on the induced drag).

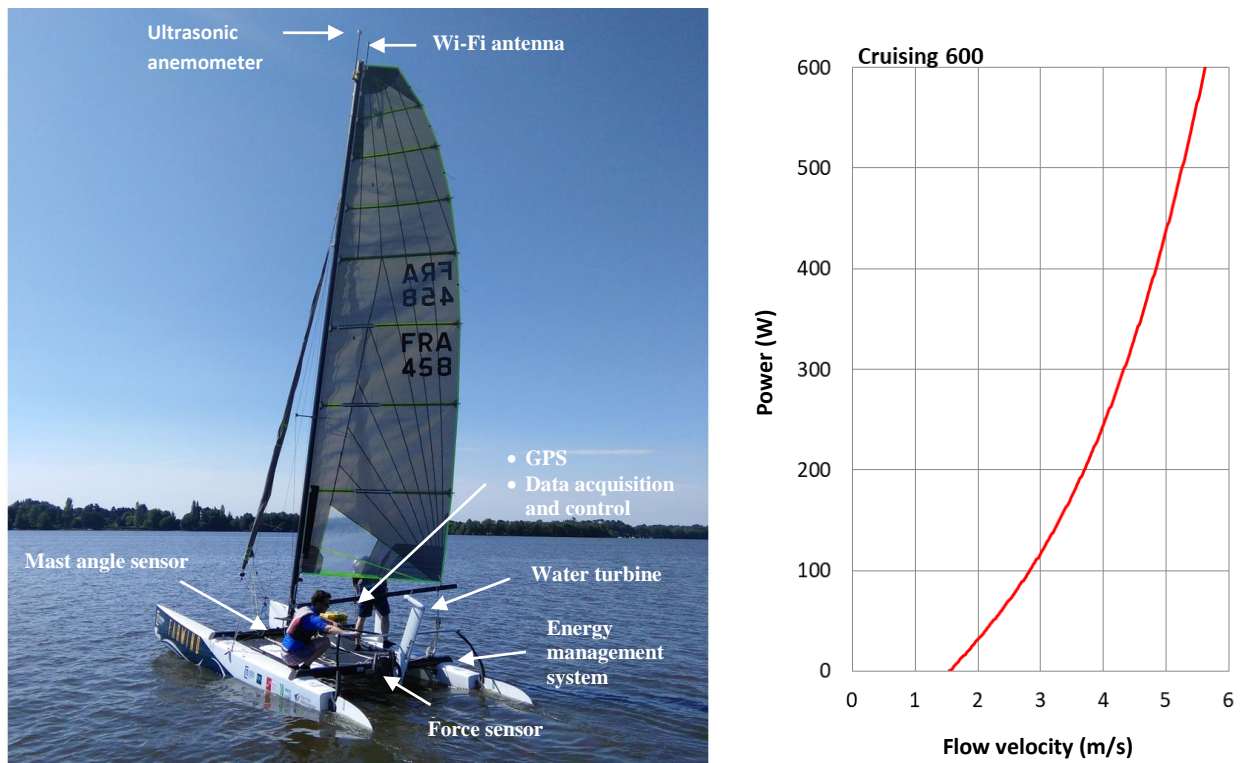
45 The aim of the present study is two-fold. First, it aims to achieve an experimental proof-of-concept  
46 of the energy ship. Indeed, to our best knowledge, all studies carried out so far are desktop studies or  
47 based on numerical models. In this respect, we believe that it is of uttermost importance to validate  
48 experimentally that significant amounts of energy can be produced with energy ships. Second, the aim  
49 is to investigate experimentally the effect of drag on energy production.

50 The remainder of the paper is organized as follows. The experimental platform is described in  
51 section 2. The tests and the experimental results are presented in section 3. Finally, in section 4, the  
52 energy performance of large-scale energy ships is extrapolated from the experimental data.

## 53 **2 Description of the experimental platform**

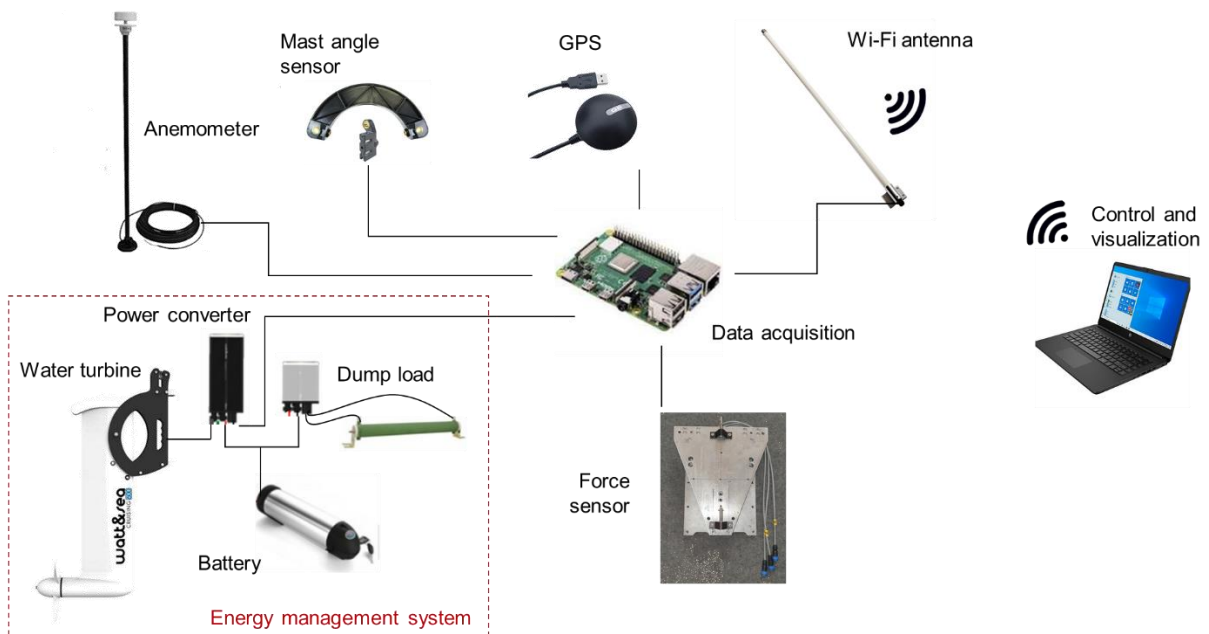
### 54 **2.1 General arrangement**

55 A second-hand Hobie Cat Tiger catamaran served as the base for the experimental platform (Figure  
56 2). Her length is 5.51 m (18 feet). The rig consists of a 17 m<sup>2</sup> mainsail and a 4.15 m<sup>2</sup> jib. It has been  
57 designed to be handled by a crew of two people. This type of catamaran was selected for its low water  
58 resistance (which is essential to maximize energy production [5][10]), its low cost on the second-hand  
59 market, and because it fairly corresponds to a 1:14 scale version of the energy ship design described  
60 in [10].



62 *Figure 2. Left: picture of the experimental platform. Right: performance of the Watt & Sea*

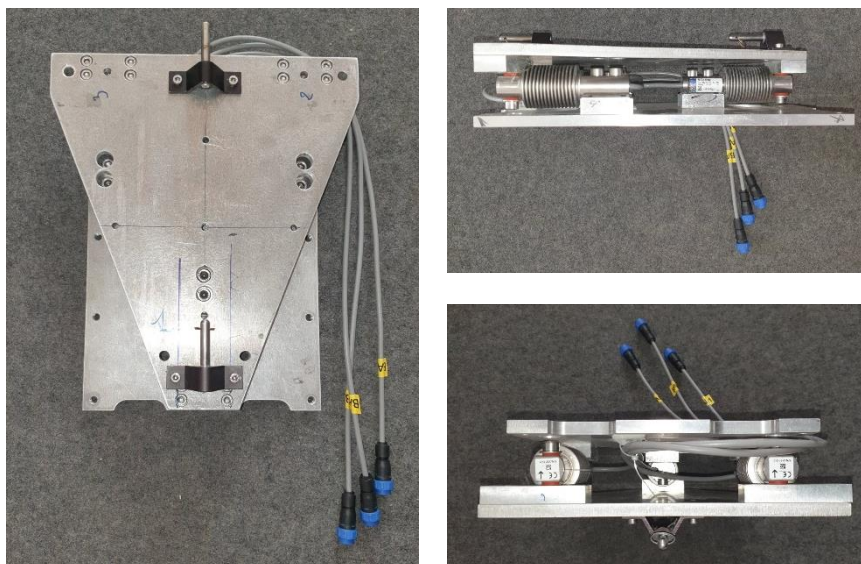
63 *Cruising 600 water turbine*



65 *Figure 3. Synoptic view of the instrumentation and equipment*

66 Figure 3 shows a synoptic view of the instrumentation and equipment which have been installed.  
67 A Watt & Sea Cruising 600 hydro-generator [13] was used for the water turbine. It has been mounted  
68 at the middle of the rear beam. The propeller diameter is 240 mm. According to the supplier, this  
69 configuration allows the production of 250 W of electrical power at a vessel speed of 4 m/s (Figure 2).

70 One of the objectives of the experimental campaign being to investigate the relationship between  
71 the drag induced by the water turbine and the energy production, a custom force sensor has been  
72 installed between the hydro-generator and the hull. The force sensor was designed and built at LHEEA  
73 (Figure 4). It consists of three HBM Z6 strain gauges mounted between two aluminum plates.  
74 Calibration results show that its accuracy is 0.4% of the maximal force (100 N).



75 *Figure 4. Force sensor*

76 The energy management system has been integrated inside the starboard float. It includes a  
77 converter which controls the generator of the water turbine, a battery, and a discharge resistor (which  
78 was included to avoid overload in case of excess energy). The energy management system includes  
79 sensors to measure the energy production (voltage, current, power) and the rotational velocity of the  
80 water turbine. The resistive torque generated by the generator at the shaft of the propeller ( $P_{shaft}$ ) is  
81 estimated from the measurement of the output current of the generator.

82 To measure the wind, a CV7-LCJ ultrasonic anemometer was installed at the top of the mast. As  
83 the Hobie Cat Tiger is equipped with a rotating wing mast, a mast angle sensor was positioned at the  
84 bottom of the mast in order to be able to correct the wind angle measurement.

85 The control and data acquisition system is based on a Raspberry Pi 3. It is integrated in a waterproof  
86 case (Pelicase) on the starboard float deck. It is connected to the various sensors by wire links. The  
87 acquisition software was developed at LHEEA in Python. It allows the continuous recording and storage  
88 of the measured data in an ASCII file in a memory card on board the platform, as well as the broadcast  
89 of the data through Wi-Fi (a Wi-Fi antenna was installed at the top of the mast). This feature allowed  
90 the experiments to be monitored and controlled in real-time by a team which stayed on the riverbank.  
91 In particular, the output voltage of the generator of the water turbine (and therefore the drag, see  
92 following section) was controlled remotely, which allowed the crew on board the catamaran to focus  
93 on navigation.

## 94 **2.2 Water turbine calibration**

95 The generator output voltage of the water turbine is controlled by the converter of the energy  
96 management system. This allows controlling the generator current and therefore the resistive torque  
97 on the shaft of the propeller, thus the propeller rotational velocity, thus the induced drag and energy  
98 production.

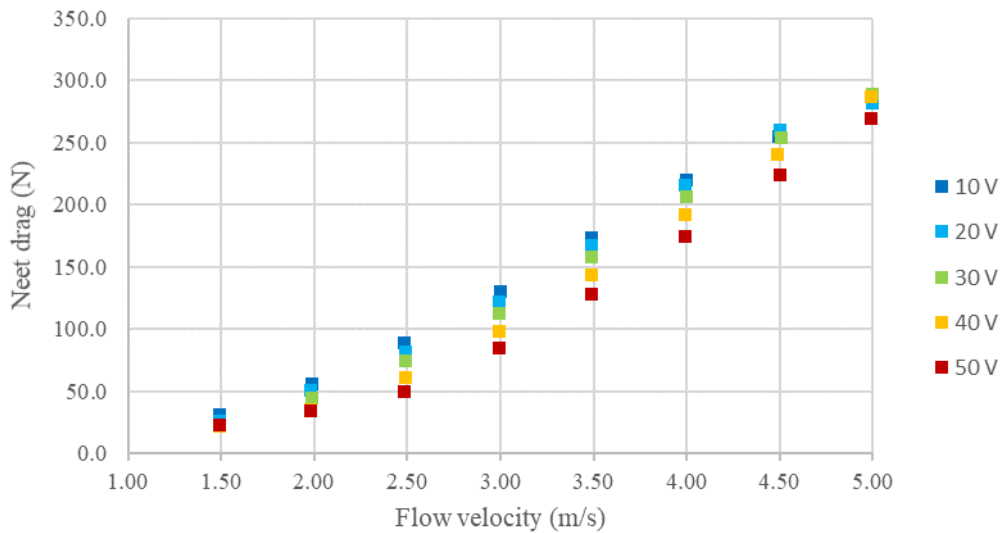
99 By default, the controller of the converter automatically optimizes the generator output voltage in  
100 order to extract the maximum power from the water turbine. For the experiments, it was modified in  
101 order to enable a given value of the generator output voltage to be prescribed (and thus the water  
102 turbine drag force).

103 To determine the characteristics of the water turbine (drag force and generated power as function  
104 of the generator setting and flow velocity), experiments were carried out in the towing tank of Ecole  
105 Centrale de Nantes. The experimental setup is shown in Figure 5. The water turbine and its force sensor  
106 were mounted on the carriage. The propeller shaft was submerged 520 mm deep. Tests were carried

107 out for a range of carriage velocities of 1.5 - 6.0 m/s. The generator output voltage was varied in the  
 108 range 10 to 50 V. The drag force was measured using the same sensor as that used for the experimental  
 109 platform (Figure 4).



110 *Figure 5. Experimental set-up for the characterization of the water turbine*



111  
 112 *Figure 6. Water turbine’s net drag force as function of the flow velocity and generator output*  
 113 *voltage.*

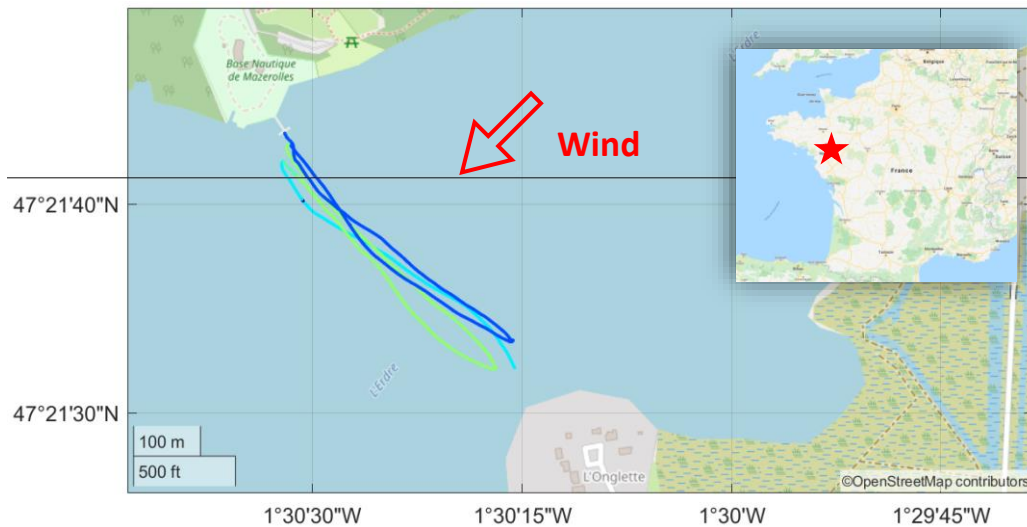
114 Figure 6 shows the measured water turbine net drag force as function of the flow velocity and  
 115 generator output voltage. The net drag force is the measured drag force minus the measured drag  
 116 force without the propeller. One can see that, as expected, the drag force decreases with increasing  
 117 output voltage. However, the controllability of the drag force appears to be limited as, for a given flow  
 118 velocity, the minimum drag force (which is obtained for an output voltage of 50 V) is at least 56% of  
 119 the maximum drag force (obtained for output voltage 10 V).

120 **3 Experiments**

121 Tests were carried out on July 2<sup>nd</sup>, 2019 at Plaine de Mazerolles on the Erdre river (France). At this  
122 location, the river is wide, and the current is negligible. The wind conditions were light (1 to 7 m/s).

123 **3.1 Method**

124 The experimental method consisted of a series of roundtrips on beam reach (see example in  
125 Figure 7). This wind direction was chosen because it corresponds to the point of sail for which the  
126 performance of energy ship is maximum [10]. On each round trip, the control setting (generator output  
127 voltage) was changed in order to study its effect on energy production. Eventually, four usable data  
128 records were obtained (labelled Run02, Run03, Run04, Run05, See Figure 7). Of these four recordings,  
129 a total of seventeen crossings of the river were made.



130

131 *Figure 7. Example of GPS trajectories during the experiments. The colors indicate the setting*  
132 *(output voltage) of the generator of the water turbine. Background picture and map:*

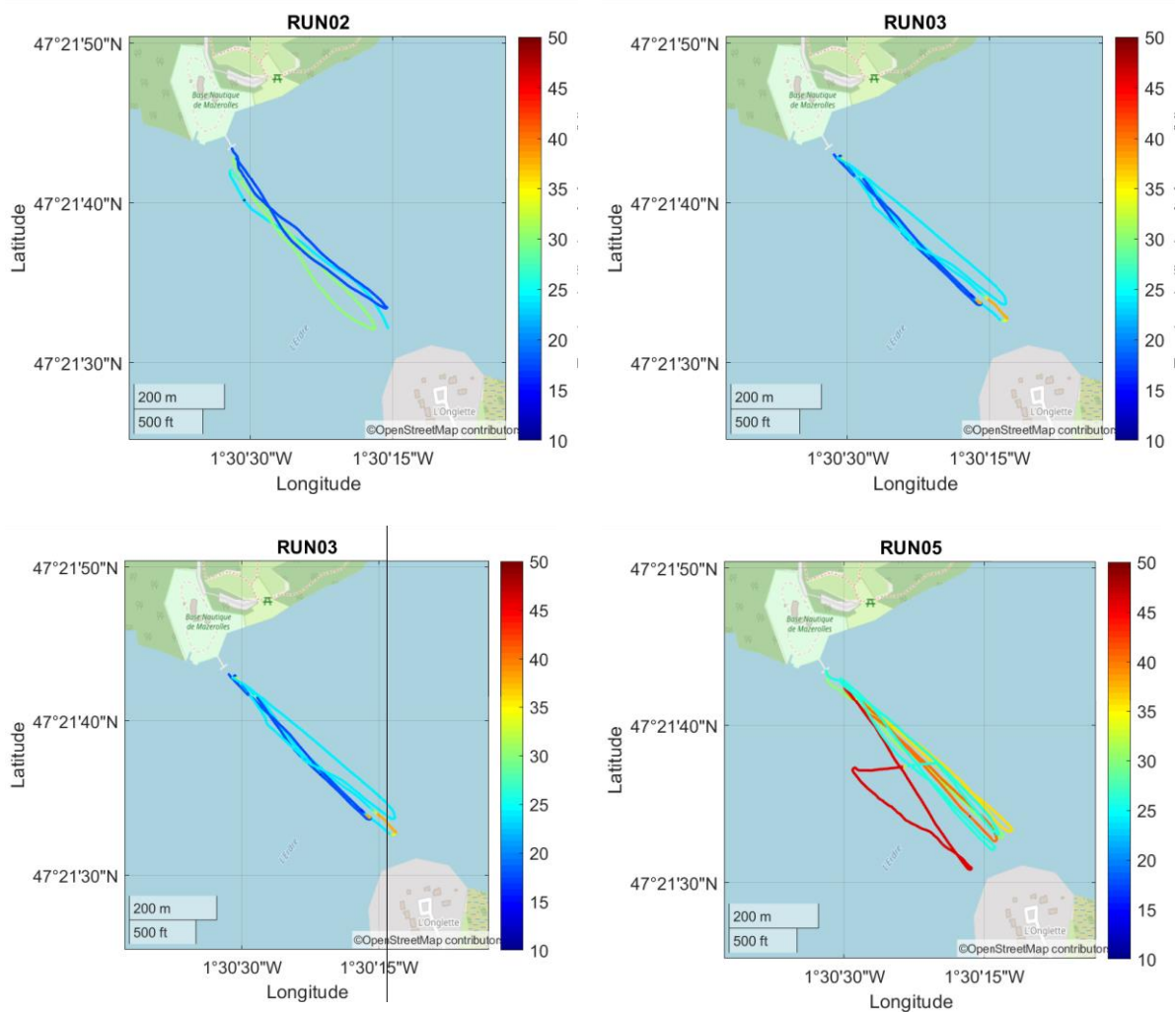
133 *OpenStreetMap*

134 **3.2 Data processing**

135 Figure 9 shows the time recording of some of the data collected during Run02 (true wind speed,  
136 boat velocity, generator output voltage, true wind angle). One can see that there are significant  
137 oscillations. They are related on the one hand to the inability of the crew to perfectly maintain heading,

138 but also and above all also to significant variations in the wind (both in strength and direction) over  
139 the test area (inland waters).

140 The seventeen river crossings were analyzed one by one in order to identify measurement  
141 intervals during which the experimental signals were stable (shaded areas in Figure 9). The signals were  
142 then averaged over each of these intervals. Standard deviations were also calculated in order to keep  
143 trace of the data quality.



144 *Figure 8. GPS traces of the experiments. The colors indicate the setting (output voltage) of the*  
145 *generator of the water turbine. Background picture: OpenStreetMap*

146 Based on the processed data, the water turbine drag coefficient  $C_T$  and the energy ship power  
147 coefficient  $C_P$  were calculated. For the water turbine drag coefficient, we used the usual definition:

148

$$C_T = \frac{D_{net}}{\frac{1}{2}\rho_{water}A_{WT}SOG^2}$$

149

(1)

150 where  $D_{net}$  is the net water turbine drag force (measured drag force minus drag force on the water

151 turbine mast),  $A_{WT}$  is the water turbine disc surface area, and  $SOG$  is the boat velocity.

152 For the power coefficient  $C_P$ , the usual definition for a water turbine is:

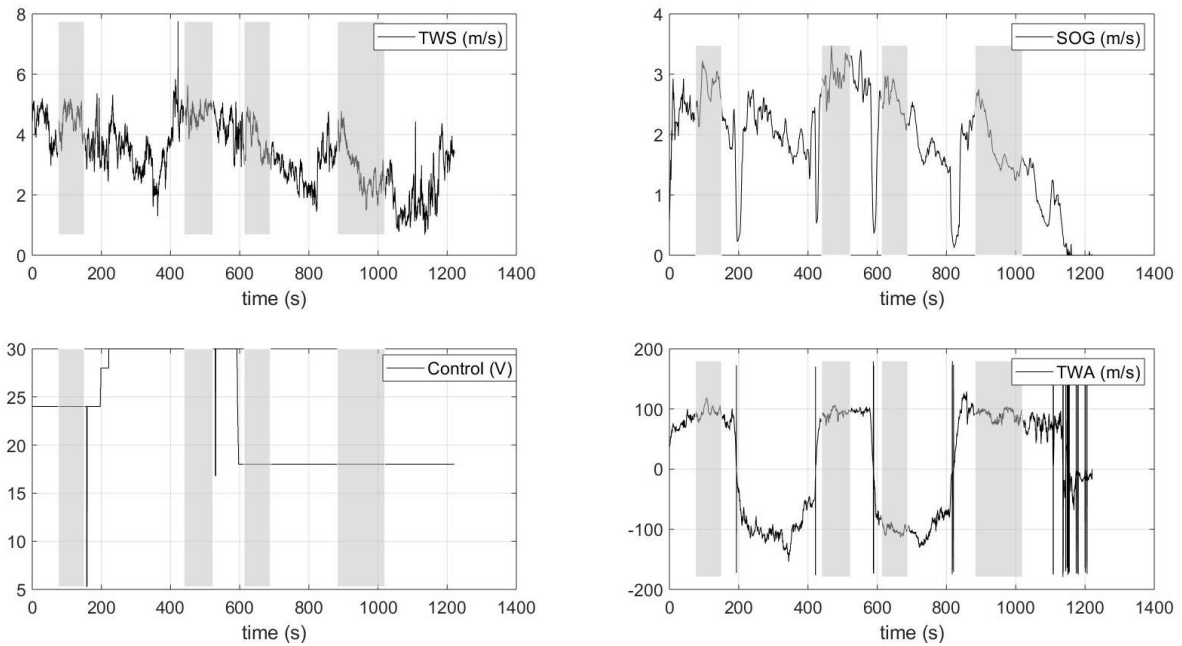
153

$$C_P = \frac{P_{shaft}}{\frac{1}{2}\rho_{water}A_{WT}SOG^3}$$

154

(2)

155 where  $P_{shaft}$  is the mechanical power at the shaft of the water turbine generator.



156

157 *Figure 9. Example of raw data measured Run02. Top left panel: true wind speed. Top right*

158 *panel: boat speed. Bottom left: generator output voltage. Bottom right: true wind angle. The*

159 *shaded areas correspond to the time windows which were retained for analysis.*

160 However, we think that this definition is not appropriate for the energy ship because it is not

161 based on the actual energy source (which is the wind). Therefore, for an energy ship, we instead

162 propose to define the power coefficient as:

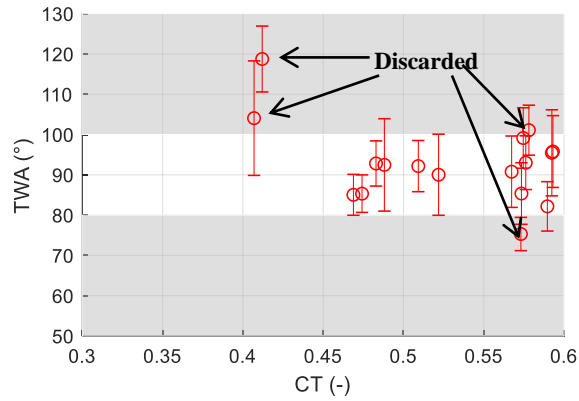
163

$$\tilde{C}_P = \frac{P_{shaft}}{\frac{1}{2}\rho_{air}A_sTWS^3}$$

164

(3)

165 where  $A_s$  is the sail area (21.15 m<sup>2</sup> in the experiments).



166

167 *Figure 10. Illustration of the data obtained after analysis. The figure shows the average true*

168 *wind angle as function of the water turbine drag coefficient.*

169 Figure 10 shows an example of the data obtained after processing. One can see that despite

170 the crew made their best effort to keep the true wind angle close to 90 degrees during the

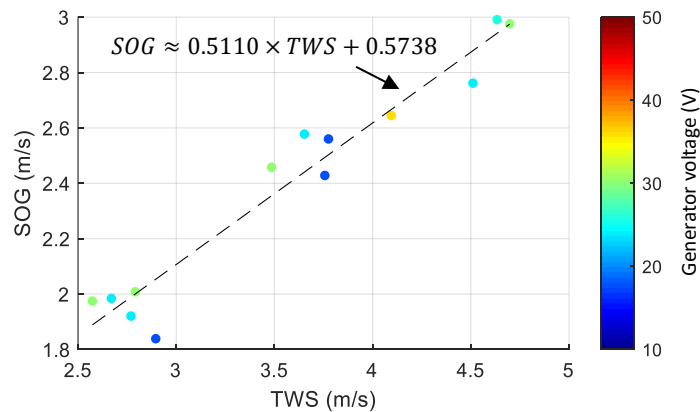
171 experiments, there are data points that deviate significantly from this objective. Since the true wind

172 angle is a key driver of energy ships' velocity and energy performance [10], and since the aim of the

173 paper is to investigate the effect of the water turbine's drag force on performance, only the data for

174 which the average true wind angle is between 80 ° and 100 ° is retained in what follows.

175



176 *Figure 11. Boat velocity (SOG) as function of the true wind speed (TWS) and generator output*  
 177 *voltage. The water turbine was in operation.*

178 Figure 11 shows the average boat velocity as function of the average true wind speed and the  
 179 generator output voltage. The range of average wind speed is 2.5 - 5.0 m/s. It appears that, when the  
 180 water turbine is in operation, the boat speed is approximately equal to half the true wind speed.  
 181 Unfortunately, no recording of the boat speed without the water turbine was made. Nevertheless, it  
 182 is typical for a sport boat (such as the catamaran used in the experiments) sailing at a 90 degrees true  
 183 wind angle that its speed is in the order of the true wind speed (if not exceeding).

### 184 3.3 Results

185 Table 1 summarizes the results of the data processing. The data for each row corresponds to the  
 186 average of the raw data over the intervals selected for analysis (see Figure 9).

187 Figure 12 shows the drag coefficient and power coefficient as function of the output voltage. In  
 188 the left panel, one can see that the drag coefficient decreases with increasing voltage (as observed in  
 189 the towing tank experiments). Note also that the range of variation of the drag coefficient is relatively  
 190 limited as it drops by only 20% when the output voltage goes from 18 to 36 V. If the full range of  
 191 variation of the voltage had been used (10 to 50V), the drag coefficient could have varied by about  
 192 40%

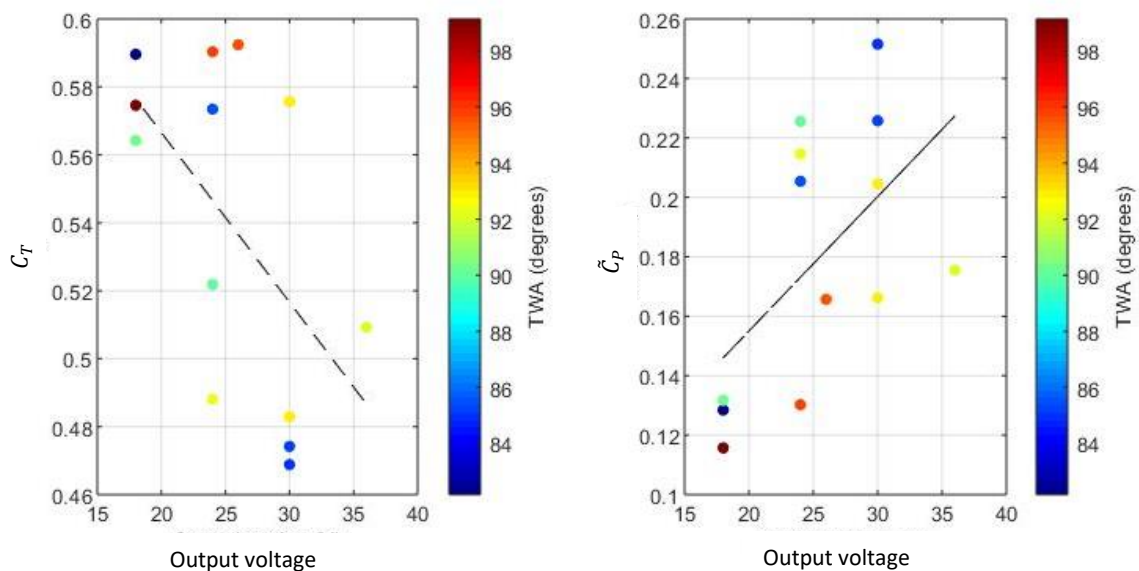
Crossing	Run number	TWS (m/s)	TWA (°)	SOG (m/s)	Output voltage (V)	$C_T$	$\tilde{C}_P$
1	3	3.77 (0.20)	82.2 (6.1)	2.56 (0.14)	18	0.590 (0.034)	0.138 (0.027)
2	4	2.57 (0.43)	85.0 (5.1)	1.97 (0.21)	30	0.469 (0.053)	0.272 (0.100)
3	4	2.79 (0.48)	85.3 (4.7)	2.01 (0.14)	30	0.474 (0.057)	0.238 (0.086)
4	3	3.65 (0.63)	85.4 (7.6)	2.58 (0.29)	24	0.573 (0.058)	0.221 (0.083)
5	3	2.77 (0.63)	90.0 (10.0)	1.92 (0.27)	24	0.522 (0.050)	0.226 (0.144)
6	2	2.90 (0.74)	90.8 (8.9)	1.84 (0.44)	18	0.567 (0.071)	0.143 (0.512)
7	5	4.10 (0.29)	92.2 (6.4)	2.64 (0.23)	36	0.509 (0.052)	0.195 (0.048)

8	3	2.67 (0.53)	92.5 (11.5)	1.98 (0.37)	24	0.488 (0.056)	0.224 (0.100)
9	5	3.49 (0.25)	92.8 (5.6)	2.46 (0.15)	30	0.483 (0.044)	0.224 (0.046)
10	2	4.70 (0.59)	93.0 (6.7)	2.98 (0.22)	30	0.576 (0.051)	0.186 (0.046)
11	5	4.63 (0.95)	95.5 (10.7)	2.99 (0.47)	26	0.592 (0.045)	0.180 (0.050)
12	2	4.51 (0.43)	95.8 (8.9)	2.76 (0.28)	24	0.593 (0.045)	0.142 (0.037)
13	3	3.76 (0.64)	99.1 (7.5)	2.43 (0.35)	18	0.575 (0.048)	0.120 (0.033)

193 *Table 1. Experimental results. The numbers between parenthesis are the standard deviations.*

194 In the right panel, one can see that, as expected, varying the output voltage - and therefore the  
 195 drag - influences energy production. For the range of tested voltage, the power output appears to  
 196 increase with increasing voltage (and thus decreasing water turbine drag). Unfortunately, the  
 197 experimental results do not allow to determine what is the optimal drag value (since the maximum  
 198 production is obtained for the upper bound of the test interval). Further testing with higher voltage  
 199 would be necessary.

200



201 *Figure 12. Drag and power coefficient of the water turbine as function of the generator output*  
 202 *voltage and true wind angle (TWA).*

## 203 4 Energy performance of a large-scale energy ship

### 204 4.1 Estimate based on the experimental data.

205 Based on the experimental results, let us estimate the energy performance of a large-scale energy  
 206 ship. It is assumed that the scale of the experiments is 1:14, as for this scale the length of the 1:1 ship  
 207 would be 77 m which is close to that of the energy ship design shown in Figure 1 (80 m). It is further  
 208 assumed that the design of the water turbine of the large-scale energy ship has the same  
 209 hydrodynamic characteristics (drag coefficients, power coefficients) as that of the water turbine used  
 210 in the experiments. Finally, the estimate is based on the data of crossing #3 in Table 1 despite crossing  
 211 #2 has the best power coefficient  $\tilde{C}_p$ , because the latter looks like an outlier.

		Experiments (1:14 scale)	1:1 scale
Length	<i>m</i>	5.51	77
Sail area	<i>m</i> <sup>2</sup>	21.15	4 145
Displacement (estimate)	<i>kg</i>	350	960 000
Wetted surface area (estimate)	<i>m</i> <sup>2</sup>	4.7	921
Water turbine diameter	<i>m</i>	0.24	3.36
$C_T$	-	0.474 (0.057)	0.474 (0.057)
$\tilde{C}_p$	-	0.238 (0.086)	0.238 (0.086)
$TWS_{10}$	<i>m/s</i>	2.79 (0.48)	7.21 (1.25)
TWA	°	85.3 (4.7)	85.3 (4.7)
SOG	<i>m/s</i>	2.01 (0.14)	7.5 (0.5)
Froude number	-	0.27	0.27
Reynolds number	-	1.1E+07	5.8E+08
Shaft power without correction (Reynolds)	<i>kW</i>	<b>0.063 (0.032)</b>	650 (330)
Shaft power with correction (Reynolds)	<i>kW</i>	N/A	<b>830 (450)</b>

212 *Table 2. Estimate of the energy production of a full-scale energy ship based on the*  
 213 *experimental results.*

214 The estimates are presented in Table 2. The data for the 1:1 scale were obtained using Froude-  
 215 scaling except for the true wind speed at 10 m altitude ( $TWS_{10}$ ), and for the energy production.  
 216 Indeed, for the true wind speed, the direct application would give the true wind speed at 140 m

217 altitude. Because of the Earth atmospheric boundary layer, the actual value at 10 m altitude is  
218 significantly smaller. In the present study, it is estimated using the classical power law:

$$219 \quad TWS(z) = TWS_{10} \left( \frac{z}{10} \right)^{0.14}$$

220 (4)

221 where  $z$  is the altitude.

222 For the energy production (mechanical power on the shaft), two values were calculated: one  
223 without considering that the Reynolds number are different between scale 1:14 and scale 1:1, and the  
224 other taking it into account. The first case corresponds to the direct application of the Froude scale. In  
225 the second case, a correction is applied to consider the effect of scale distortion. Indeed, at the 1:14  
226 scale, the drag force of the hull can be written:

$$227 \quad R_{W,1:14} = \frac{1}{2} \rho_{water} A_{W,1:14} C_{W,1:14} U_{1:14}^2$$

228 (5)

229 where  $A_{W,1:14}$  is the wetted surface of the hull,  $C_{W,1:14}$  is the hull resistance coefficient, and  $U_{1:14}$  is  
230 the ship velocity. As the forward speed was moderate in the tests ( $F_n \sim 0.27$ ) and since the hull consists  
231 of two thin floats, the component of the hull resistance coefficient associated with wave resistance is  
232 neglected. Thus, the hull resistance coefficient reduces to its friction component  $C_{f,1:14}$ . According to  
233 ITTC [12], it can be written:

$$234 \quad C_f = \frac{0.075}{(\log_{10} Re - 2)^2}$$

235 (6)

236 The application of the ITTC formula shows that the friction coefficient is of the order of 0.0029  
237 at scale 1:14, whereas it is 0.0016 at scale 1:1. Therefore, the direct application of Froude scaling  
238 overestimates the full-scale hull resistance by up to 80%.

239 Let us then estimate energy production considering this effect. Let us denote  $\Delta R_W$  the  
 240 difference in hull resistance between that obtained using Froude scaling and that estimated  
 241 considering the full-scale Reynolds number:

$$\begin{aligned}
 242 \quad \Delta R_W &= 14^3 R_{W1:14} - \frac{1}{2} \rho S_{W,1:1} C_{W,1:1} U_{1:1}^2 \\
 243 \quad \Delta R_W &= 14^3 \left( R_{W1:14} - \frac{1}{2} \rho S_{W,1:14} C_{W,1:1} U_{1:14}^2 \right) \\
 244 & \hspace{20em} (7)
 \end{aligned}$$

245 To estimate the additional power available to the water turbine, let us consider the equation  
 246 of motion of the ship at equilibrium:

$$\begin{aligned}
 247 \quad T &= R_W + D \\
 248 & \hspace{20em} (8)
 \end{aligned}$$

249 Where  $T$  is the thrust delivered by the sails and  $D$  is the water turbine drag force. Equation 8 can be  
 250 rewritten:

$$\begin{aligned}
 251 \quad D &= T - R_W \\
 252 & \hspace{20em} (9)
 \end{aligned}$$

253 In particular, at the 1:14 scale:

$$\begin{aligned}
 254 \quad D_{1:14} &= T_{1:14} - R_{W1:14} \\
 255 & \hspace{20em} (10)
 \end{aligned}$$

256 And at scale 1:1:

$$\begin{aligned}
 257 \quad D_{1:1} &= T_{1:1} - R_{W1:1} \\
 258 & \hspace{20em} (11)
 \end{aligned}$$

259 For the thrust delivered by the sails, the Reynolds number at the 1:14 scale is of the order of  
 260  $10^5$  against  $10^6$  for scale 1:1. Thus, the air flow is fully turbulent, and we can therefore assume that  
 261 there is no effect of scale. Therefore:

262 
$$D_{1:1} = 14^3 T_{1:14} - R_{W1:1}$$

263 (12)

264 By injecting Equation 10 into Equation 12:

265 
$$D_{1:1} = 14^3 (D_{1:14} + R_{W1:14}) - R_{W1:1}$$

266 (13)

267 Finally:

268 
$$D_{1:1} = 14^3 \left( D_{1:14} + \frac{1}{2} \rho S_{W,1:14} C_{f,1:14} U_{1:14}^2 \right) - \frac{1}{2} \rho S_{W,1:1} C_{f,1:1} U_{1:1}^2$$

269 
$$D_{1:1} = 14^3 \times \frac{1}{2} \rho \left( \frac{\pi}{4} D_{1:14}^2 C_T + S_{W,1:14} (C_{f,1:14} - C_{f,1:1}) \right) U_{1:14}^2$$

270 (14)

271 The numerical application of this latter equation shows that the drag induced by the water  
 272 turbine must be increased by 28% for the speed of the ship at scale 1:1 to correspond to that of the  
 273 ship at scale 1:14. The power production being proportional to the water turbine drag, it is also  
 274 increased by 28%. Thus, by a wind of force 4 (7.2 m/s) on the Beaufort scale, the 1:1 scale energy ship  
 275 may therefore be capable of producing over 800 kW.

276 **4.2 Estimate based on a numerical model validated against the present experiments.**

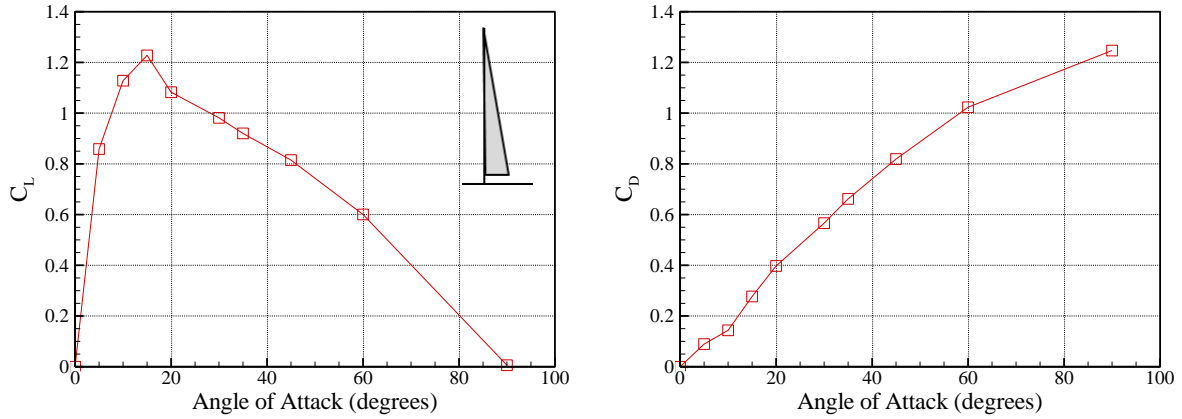
277 Another approach to estimate the energy performance of a large-scale energy ship is to use a  
 278 numerical model. In such approach, the experimental results are used to validate the model. Then, the  
 279 model can be used to determine the velocity and power performance at large scale.

280 In the present study, the numerical model is based on that presented in [10]. That model requires  
 281 as inputs the characteristics of the rig (dimensions, aerodynamic coefficients), of the hull (dimensions  
 282 and residuary coefficients) and of the water turbine.

283 As mentioned previously, the rig of the Hobie Cat Tiger consists of a mainsail (17 m<sup>2</sup>) and a jib  
 284 (4.15 m<sup>2</sup>). Unfortunately, to our knowledge, the aerodynamic coefficients for this exact configuration

285 are not available in the literature. Therefore, we used as an approximation the aerodynamic  
286 coefficients of a mainsail of aspect ratio 6 (Figure 13).

287

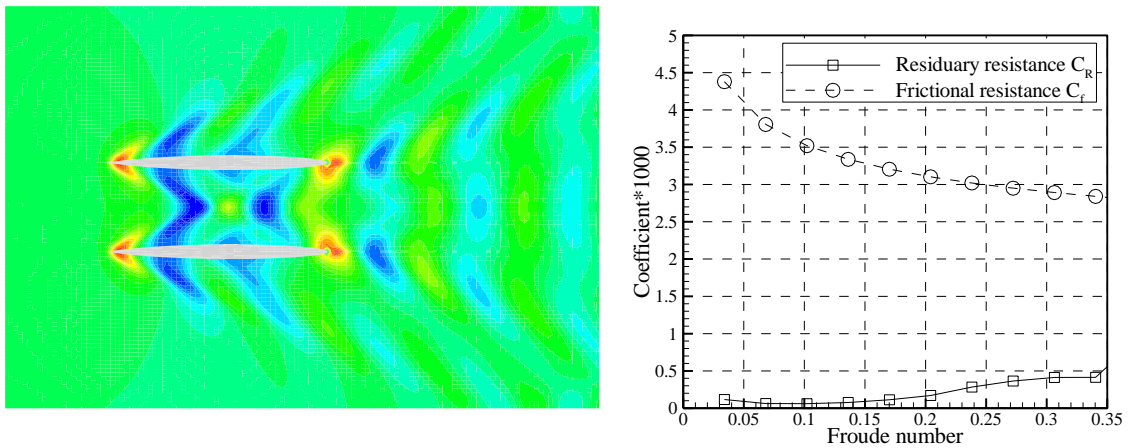


288 *Figure 13. Lift (left) and drag (right) coefficients of a Bermudan sail of aspect ratio 6. Source:*

289

*Figure 127 in [14]*

290 The hull was 3D-scanned in order to achieve a digital-twin. Her estimated displacement during the  
291 experiments is 350 kg (light ship: 180 kg, crew: 150 kg, force sensor: 6kg, water turbine: 9 kg, other  
292 sensors and equipment: 5 kg). For that displacement, the hull wetted surface is 4.7 m<sup>2</sup>. The hull  
293 residuary resistance coefficients were obtained using the REVA software [15] (Figure 14).



294

295 *Figure 14. Left: Picture of the wave field for ship velocity 2 m/s (Froude number 0.272). Right:*

296

*hydrodynamic coefficients.*

297 To accurately estimate the water resistance, it is also important to take into account the  
 298 appendages. In this respect, the Hobie Cat Tiger is equipped with two daggerboards (0.55 m<sup>2</sup>) and two  
 299 rudders (0.15 m<sup>2</sup>). They were modelled as NACA 0009 profile.

300 For the water turbine coefficients, the results obtained in the towing tank experiments were used  
 301 (see section 2.2).

302 Table 1 shows the comparison of the experimental results and of the numerical model for wind  
 303 conditions corresponding to crossing #3 ( $TWS_{10} = 10$  m/s, TWA = 85.3°). The velocity predicted by  
 304 the numerical model is 2.15 m/s, which is 7% greater than in the experiments (while falling in the  
 305 uncertainty range). The predicted power is 69 W, thus 10% greater than in the experiments. Therefore,  
 306 the agreement between the numerical model and the experiments is very good.

		1 :14 scale		1 :1 scale	
		Experiments	Numerical model	Scaled water turbine	Optimized water turbines
<b>Length</b>	<i>m</i>	5.51	5.5	77	77
<b>Sail area</b>	<i>m</i> <sup>2</sup>	21.15	21.15	4 145	4 145
<b>Displacement</b>	<i>kg</i>	350 (estimate)	350	960 000	960 000
<b>Wetted surface area</b>	<i>m</i> <sup>2</sup>	4.7 (estimate)	4.7	921	921
<b>Water turbine diameter</b>	<i>m</i>	0.24	0.24	3.36	4.
$C_T$	-	0.474 (0.057)	0.474	0.474	0.274
$TWS_{10}$	<i>m/s</i>	2.79 (0.48)	2.79	10.	10.
<b>TWA</b>	°	85.3 (4.7)	85.3	90	90
<b>SOG</b>	<i>m/s</i>	2.01 (0.14)	2.15	10.75	9.61
<b>Froude number</b>	-	0.27	0.30	0.39	0.35
<b>Reynolds number</b>	-	1.1E+07	1.2E+07	8.2E+08	7.4E+08
<b>Shaft power</b>	<i>kW</i>	0.063 (0.032)	0.069	1 690	2 320

307 *Table 1. Comparison of the experimental results and the numerical results at 1:14 scale, and*  
 308 *estimates of power production of a large-scale energy ship with the scaled water turbine and*  
 309 *optimized water turbines.*

310 Table 1 also shows velocity and power performance results for the large-scale energy ship. Note  
311 that for the large-scale ship, it is assumed that the sail area is distributed over two masts of height 90  
312 m each. This is because the total sail area of the 1:1 ship is 4 145 m<sup>2</sup>, which is 73% more than the world  
313 greatest Bermudan rig (2 385 m<sup>2</sup>, [16]). Thus, 45 m has been used for the reference altitude for the  
314 calculation of the wind speed in Equation 4 (instead of 63 m for the direct application of the Froude-  
315 scale).

316 Two versions of the large-scale scale energy ship were considered. In the first one (scaled water  
317 turbine), it is assumed that the ship is equipped with a water turbine whose hydrodynamic coefficients  
318 are the same as in the experiments (as in the previous section). According to the model, that ship  
319 would sail at a velocity of 10.75 m/s (almost 21 knots) and it could deliver 1 690 kW of mechanical  
320 power on the shaft of the generator for a true wind speed of 10 m/s at 10 m altitude and a true wind  
321 angle of 90 degrees.

322 In the second version, it is assumed that the ship is equipped with two water turbines of 4 m  
323 diameter, and that the design of the rotor of the turbines is optimized. Indeed, it was shown in Pelz et  
324 al. [5] that a key parameter for maximizing energy recovery is the drag induced by the water turbine,  
325 and that the optimal drag can be significantly different from that for wind turbines or tidal turbines  
326 [10]. Therefore, in the present study, it is assumed that the water turbine's rotor is such that it can  
327 deliver the same thrust and power as an actuator disc with 80% efficiency, and the induction factor is  
328 optimized in order to maximize power. Results show that that ship could produce 2 320 kW for a true  
329 wind speed of 10 m/s and a true wind angle of 90°. Thus, despite sailing slower than the ship with the  
330 scaled water turbine, it would produce 37% more power. This can be explained by the significantly  
331 smaller induction factor of the turbines' rotors which minimizes the hydrodynamic losses (see section  
332 2.2 in [10]).

333 Finally, in agreement with [10], it appears that power production of order of a few megawatts is  
334 feasible for large-scale energy ships for wind conditions of force 5 on the Beaufort scale, wind  
335 conditions which are very common in the high seas.

## 336 **5 Conclusion**

337 In this paper, we presented an experimental proof-of-concept of the energy ship concept. It is  
338 based on a 5.5 m long sailing catamaran equipped with a 600 W hydro-generator. A power production  
339 (mechanical power) of 63 W was measured in the experiments for a true wind speed of 2.79 m/s and  
340 a true wind angle of 85.3°. It corresponds to approximately 2 MW for a wind of force 5 on the Beaufort  
341 scale for a large-scale energy ship. Thus, the experiments confirm that the energy ship concept can  
342 lead to power production levels comparable to wind turbines.

343 The experimental results also confirm the importance of optimizing the water turbine drag to  
344 maximize power production. However, unfortunately, it was not possible to determine the optimum  
345 drag in the experiments as it is out of the range achievable by the used water turbine. This issue may  
346 be addressed in future work. Note that it may require the development of new water turbine rotor's  
347 designs dedicated to energy ships as their optimal induction factor may be significantly different than  
348 that of wind turbines or tidal turbines.

## 349 **Acknowledgements**

350 This work was supported by the Pays de la Loire Region, France; and Nantes Métropole, Nantes, France  
351 [WEAMEC project WEREVER\_DEMO].

## 352 **References**

353 [1] Babarit, J-C. Gilloteaux, E. Body, J-F. Hétet (2019) Energy and economic performance of the  
354 FARWIND energy system for sustainable fuel production from the far-offshore wind energy  
355 resource. In Proc. Of the 14th International Conference on Ecological Vehicles and Renewable  
356 Energies (EVER), Monaco

- 357 [2] R.E. Salomon (1982) Process of converting wind energy to elemental hydrogen and apparatus  
358 therefore. U.S. Patent 4335093A
- 359 [3] J. Kim, C. Park (2010) Wind power generation with a parawing on ships, a proposal. *Energy*,  
360 Vol. 35, pp. 1425-1432
- 361 [4] A. Babarit, J.C. Gilloteaux, G. Clodic, M. Duchet, A. Simoneau, M.F. Platzer (2018) Techno-  
362 economic feasibility of far offshore hydrogen-producing wind energy converters. *International*  
363 *Journal of Hydrogen Energy*, Vol. 43(15), pp. 7266-7289
- 364 [5] P.F. Pelz, M. Holl, M. Platzer (2016) Analytical method towards an optimal energetic and  
365 commercial wind-energy converter. *Energy*, Vol. 94, pp. 344-351
- 366 [6] M.F. Platzer, N. Sarigul-Klijn, J. Young, M.A. Ashraf, J.C.S. Lai (2014) Renewable hydrogen  
367 production using sailing ships. *ASME Journal of Energy Resources Technology*, Vol. 136
- 368 [7] M. Tsujimoto, T. Uehiro, H. Esaki, T. Kinoshita, K. Takagi, S. Tanaka, H. Yamaguchi, H. Okamura,  
369 M. Satou, Y. Minami (2009) Optimum routing of a sailing wind farm. *Journal of Marine and*  
370 *Science Technology*, Vol. 14, pp. 89-103
- 371 [8] K. Ouchi, J. Henzie (2017) Hydrogen generation sailing ship: conceptual design and feasibility  
372 study. In *Proc. of IEEE OCEANS 2017*
- 373 [9] J.C. Gilloteaux, A. Babarit (2017) Preliminary design of a wind driven vessel dedicated to  
374 hydrogen production. In *Proc. of the ASME 36th International Conference on Ocean, Offshore*  
375 *and Arctic Engineering (OMAE2017)*, Trondheim, Norway.
- 376 [10] A. Babarit, G. Clodic, S. Delvoye, J-C. Gilloteaux (2020) Exploitation of the far-offshore wind  
377 energy resource by fleets of energy ships. Part A. Energy ship design and performance. *Wind*  
378 *Energy Science*, Vol. 5, pp. 839-853
- 379 [11] R. Abd-Jamil, A. Chaigneau, J-C. Gilloteaux, P. Lelong, A. Babarit (2019) Comparison of the  
380 capacity factor of stationary wind turbines and weather-routed energy ships in the far-  
381 offshore. *Journal of Physics: conference series*, Vol. 1356

- 382 [12]ITTC: General guidelines for uncertainty analysis in resistance tests. ITTC – Recommended  
383 procedures 7.5-02-02-02, 2014
- 384 [13]<https://www.wattandsea.com/fr/produits/hydro-cruising/hydro-cruising-600>
- 385 [14]C.A. Marchaj (2010) Sail performance: techniques to maximise sail power. Adlard coles  
386 nautical, London, UK.
- 387 [15]G. Delhommeau, J-J. Maisonneuve (1987) Extensions du code de calcul de résistance de vagues  
388 REVA: prise en compte des effets de fond et de portance. Compte rendu des 1ères journées  
389 de l’hydrodynamique, Nantes, 1987
- 390 [16] [https://en.wikipedia.org/wiki/Mirabella\\_V](https://en.wikipedia.org/wiki/Mirabella_V)